Theoretical calculation of the thickness of interphase zones in the Al-Al2O3 composite

O.A. Pashkov[1]

[1]Moscow Aviation Institute (National Research University), Volokolamskoe shosse, 4, 125993, Moscow, Russia
[1]oapashkov@mail.ru

Article History Received: 10 January 2021; Revised: 12 February 2021; Accepted: 27 March 2021; Published online: 28 April 2021

Abstract: In the work, a theoretical study of the mechanical characteristics of the composite of the Al-Al_2O_3 system. The substantiation of the lowered values of the strength of the composite specimens is proposed, :interphase zone (for which the composition and approximate thickness is determined) on the mechanical properties of the material has been carried out; it is shown that, within the framework of the classical model of multilayer cylindrical fibers, the resulting interfacial zones do not significantly affect the properties of the material, but the level of residual stresses can be affected.

Keywords: Composite materials, strength, interfacial layer, aluminum oxide.

1. Introduction

Modern composites have not only a wide range of physical and mechanical properties, but are also capable of directionally changing them, for example, increasing fracture toughness, regulating rigidity, strength, and other properties [1-12]. These possibilities are expanded when fibers of different nature and geometry are used in composites, i.e., when creating hybrid composites [13-24]. In addition, these materials are characterized by the appearance of a synergistic effect (coordinated joint action of several factors in one direction).

The properties of the interface or interfacial zone, first of all, the adhesive interaction between the fiber and the matrix, determine the level of properties of composites and their retention during operation [25-35]. Local stresses in the composite reach their maximum values just near or directly at the interface, where material destruction usually begins. The interface must have certain properties to ensure efficient transfer of the mechanical load from the matrix to the fiber [36-41]. The adhesion bond at the interface should not be destroyed under the action of thermal and shrinkage stresses arising from the difference in the temperature coefficients of linear expansion of the matrix and fiber or as a result of chemical shrinkage of the binder during its curing.

2. Calculation of the parameters of the interphase layer

To assess the interphase layer at the interface between the fibers of aluminum oxide and a matrix containing Mg, the above relation is used:

$$h(t) = K_0 \exp\left[-\frac{E \pm \kappa\sigma_{kk}}{2RT}\right]\sqrt{t}, \quad h(t) \equiv \delta(t)$$

where K_0 – this is a preexponential parameter determined experimentally, E – activation energy of the growth process of the reaction zone, R=8,314 – universal gas constant, T – process temperature on the Kelvin scale, σ_{kk} - ball tensor. The parameter κ is determined according to the experimental data.

The following activation energies are known for the growth processes of spinel interphase zones under study. In the studied aluminum-based composites reaction occurs:
$(3/4(Al_2O_3)+Mg \rightarrow (3/4)\underline{MgAl_2O_4}+(1/2)Al)$

The process begins at a temperature of 900 K. For it, the value of activation energy *E* = 103 kJ is known. It is important to note that in the aluminum-oxide composites aluminum for the temperature ranges under consideration there is no reaction directly between the aluminum matrix and the fibers, that is, the alumina fibers should not undergo destruction, since this process can only begin at temperatures above 900 K.

In this case, we know the only experimental point determined by the parameters:

- Temperature T = 1020 K.
- Process time t = 5 min.
- Pressure P = 130 MPa (here P is the ball stress tensor)
- The thickness of the interphase layer was: h = 20 nm.

As a result of modeling, it is required to determine the change in the width of the interphase layer, as well as to analyze its dependence on pressure and temperature, if the temperature changes in the range T = 970-1020 K

(700-750 C), the process time changes in the interval t = 1-3 minutes, and the pressure of the process is in the range P = 3000-4000 kPa (30-40 atm.).

For a composite based on an aluminum alloy containing magnesium alloying additives and reinforced with aluminum oxide fibers, it is known that diffusion processes resulting in the formation of spinel (3/4(Al_2O_3)+Mg -> (3/4)$MgAl_2O_4$+(1/2)Al) begin at a temperature of 900 K. For such a process, the following parameters are known:

- K_0 = 7,07 nm $c^{-0.5}$,
- E = 103 kJ,

First, let us determine the parameter κ keeping in mind the above experimental data. As a result, it was found that $\kappa = 0.235714$.

After determining the value κ you can establish the dependence of the thickness of the interphase layer on the holding time.

In Figure 1, such a dependence is plotted for the parameters:

K_0 = 7,07 nm $c^{-0.5}$, E = 103 kJ, T = 1020 K, P = 3000Pa,

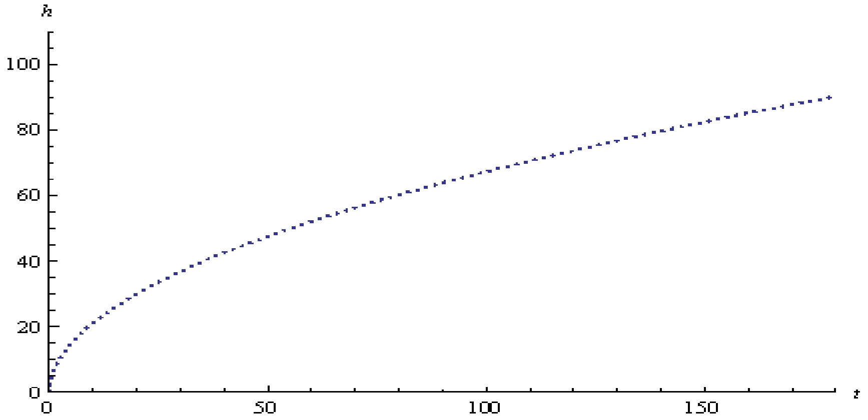

Figure 1. Dependence of the interfacial layer thickness in nanometers (K_0 = 7,07 nm c-0.5, E = 103 kJ, T = 1020 K, P = 3000Pa)

Further the influence of pressure and temperature on the rate of formation of the interphase layer is investigated.

It was found that in the specified range of these characteristics, the growth of the interphase layer does not depend on them. This is demonstrated in Figure 2, which shows the dependences for the interfacial layer thicknesses when the parameters are fixed:

K_0 = 7,07 nm $c^{-0.}$, E = 103 kJ, P = 3000 Pa.

The upper curve is plotted for temperature T=1020 K, and the lower one is for T=720 K.

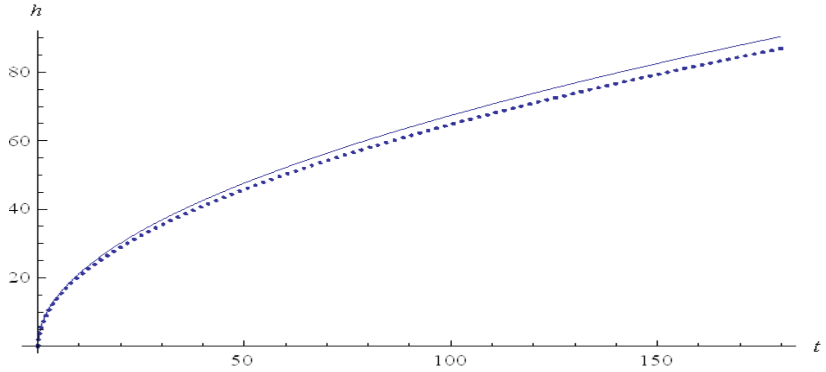

Figure 2. Assessment of the effect of temperature on the thickness of the interfacial layer (in nanometers).

Let us find out whether the accuracy of determining the activation energy affects the estimates of the interfacial layer thickness. To do this, first the parameter is determined again κ, according to the experimental test, and then the dependence of the layer thickness on the holding time is plotted.

The following activation energies are compared: 1. E = 103 kJ, 2. E = 90 kJ. It was found that for these activation energies the parameter κ does not actually change. As a result, the accuracy of setting the activation energy in the indicated ranges does not affect the estimates of the interfacial layer thickness.

Next, the influence of the parameter is estimated K_0. The following three options were compared: 1. K_0 = 7,07 nm $s^{-0.5}$, 2. K_0 = 5 nm $s^{-0.5}$, 3. K_0 = 9 nm $s^{-0.5}$.

The procedure for calculating the parameters κ was repeated again. The following values of this parameter were found for three variants: 0.2356144, 0.190418; 0.267104.

After that, the time dependences for the interphase layer were constructed. The results are shown in the Figure 3:

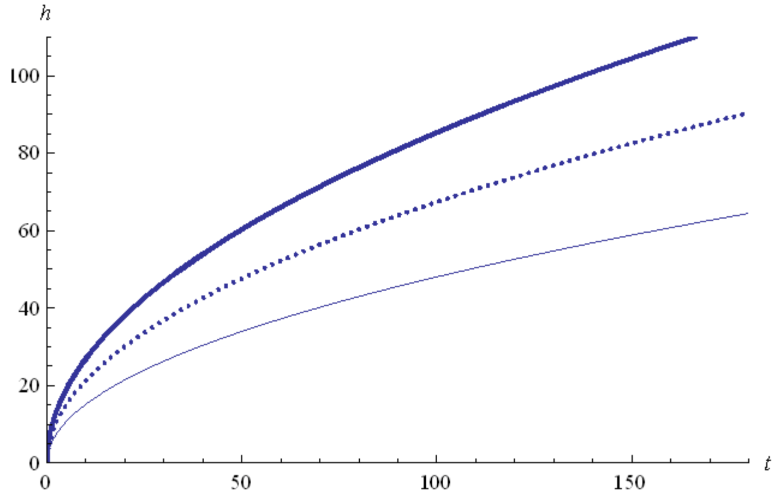

Figure 3. Influence of the accuracy of determining the parameter K_0 on the prediction of the interfacial layer thickness (solid thick line - K_0 = 9 nm $s^{-0.5}$, dotted line - K_0 = 7,07 nm $s^{-0.5}$, thin line - dotted line - K_0 = 5 nm $s^{-0.5}$.

It is important to note that the accuracy of the forecast is affected by the accuracy of determining the parameters in the formula (*). Therefore, it is very important to expand the experimental data, which can be used to determine (and refine) the parameters included in (*). Having these data and solving the problem of identifying the parameters of the model (*) by minimizing the target function (error of the theoretical dependence) in the rate selected after testing, we can significantly refine the forecast data for the thickness of the interphase layer.

According to some sources, the growth of the spinel interphase zone can begin only after the passage of the "incubation" period, which for temperatures amounts to 1000 K - 2000 s and for temperatures above 1000 K decreases to 500 s. Thus, the studied processing time is 3 min. may not be enough to start the growth of interfacial zones in the aluminum composite. Figure 4 shows the refined dependence of the thickness of the interfacial zone, depending on the temperature of the process and taking into account the incubation period. Here it was assumed that the incubation time decreases linearly with an increase in temperature from 970 to 1020 K from an initial value of 2000 s to a value of 500 s.

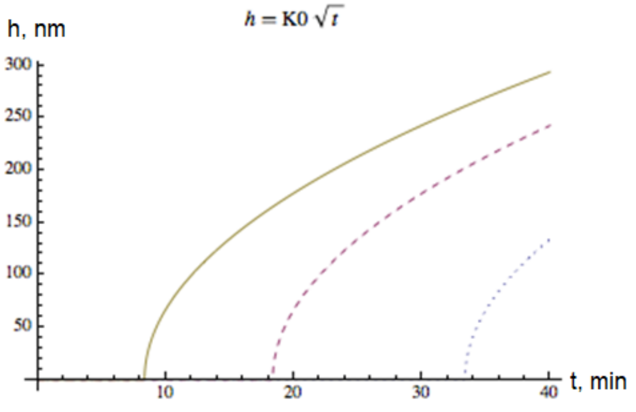

Figure 4. Dependence of the thickness of the interphase zone on time, taking into account the incubation period (solid line T = 1020K, dashed line - T = 1000 K, dotted line - T = 970K).

3. Conclusions

Modeling shows that in a given range of temperature and pressure variation, an interfacial layer thickness of 60-120 nm can be realized. At the same time, neither temperature nor pressure (in the specified ranges) has a significant effect on the thickness. Optimum thickness can only be achieved by changing the holding time. Based on the preliminary calculations (which may require clarification during the experiments), it is possible to recommend carrying out the technological process for obtaining samples at a temperature of 750 K to ensure the shortest time of the incubation period of growth. The pressure should be minimal in the selected range - 30 atm., to increase the growth rate of the interphase zone. The process time should be 10-20 minutes to obtain an interface thickness of 80-150 nm. If the phenomenon of the incubation period of the beginning of the growth of the interfacial zone is not confirmed, the holding time should be 3-5 minutes.

References

1. Dobryanskiy, V.N., Rabinskiy, L.N., Tushavina, O.V. Experimental finding of fracture toughness characteristics and theoretical modeling of crack propagation processes in carbon fiber samples under conditions of additive production// Periodico Tche Quimica, 2019, 16(33), p. 325–336.
2. Rabinskiy, L.N., Tushavina, O.V., Formalev, V.F. Mathematical modeling of heat and mass transfer in shock layer on dimmed bodies at aerodynamic heating of aircraft// Asia Life Sciences, 2019, (2), p. 897–911.
3. Antufev, B.A., Egorova, O.V., Rabinskiy, L.N. Quasi-static stability of a ribbed shell interacting with moving load// INCAS Bulletin, 2019, 11, p. 33–39.
4. Bodryshev, V.V., Babaytsev, A.V., Rabinskiy, L.N. Investigation of processes of deformation of plastic materials with the help of digital image processing// Periodico Tche Quimica, 2019, 16(33), p. 865–876.
5. Kuznetsova, E.L., Rabinskiy, L.N. Heat transfer in nonlinear anisotropic growing bodies based on analytical solution // Asia Life Sciences, 2019, (2), p. 837–846.
6. Kuznetsova, E.L., Rabinskiy, L.N. Numerical modeling and software for determining the static and linkage parameters of growing bodies in the process of non-stationary additive heat and mass transfer//Periodico Tche Quimica, 2019, 16(33), p. 472–479.
7. Formalev, V.F., Kolesnik, S.A., Selin, I.A. Local non-equilibrium heat transfer in an anisotropic half-space affected by a non-steady state point heat source // Herald of the Bauman Moscow State Technical University, Series Natural Sciences. 2018. 80(5), p. 99-111.
8. Kolesnik, S.A., Bulychev, N.A., Rabinskiy, L.N., Kazaryan, M.A. Mathematical modeling and experimental studies of thermal protection of composite materials under high-intensity effects of laser radiation// Proceedings of SPIE - The International Society for Optical Engineering. 2019. 11322, article number 113221R.
9. Kuznetsova, E.L., Rabinskiy, L.N. Linearization of radiant heat fluxes in the mathematical modeling of growing bodies by the action of high temperatures in additive manufacturing //Asia Life Sciences, 2019, (2), p. 943–954.
10. Babaytsev, A.V., Kuznetsova, E.L., Rabinskiy, L.N., Tushavina, O.V. Investigation of permanent strains in nanomodified composites after molding at elevated temperatures// Periodico Tche Quimica, 2020, 17(34), p. 1055–1067.
11. Rabinsky, L.N., Kuznetsova, E.L. Simulation of residual thermal stresses in high-porous fibrous silicon nitride ceramics // Powder Metallurgy and Metal Ceramics, 2019, 57(11-12), p. 663–669.
12. Rabinskiy, L.N. Non-stationary problem of the plane oblique pressure wave diffraction on thin shell in the shape of parabolic cylinder// Periodico Tche Quimica, 2019, 16(32), p. 328–337.
13. N.A. Bulychev, A.V. Ivanov. Effect of vibration on structure and properties of polymeric membranes, International Journal of Nanotechnology, 2019, Vol. 16, Nos. 6/7/8/9/10, pp. 334 – 343.
14. O.A. Butusova. Surface Modification of Titanium Dioxide Microparticles Under Ultrasonic Treatment, International Journal of Pharmaceutical Research, 2020, Vol. 12, I. 4, pp. 2292-2296.
15. N.A. Bulychev, A.V. Ivanov. Nanostructure of Organic-Inorganic Composite Materials Based on Polymer Hydrogels, International Journal of Nanotechnology, 2019, Vol. 16, Nos. 6/7/8/9/10, pp. 344 – 355.
16. M.O. Kaptakov. Effect of Ultrasonic Treatment on Stability of TiO2 Aqueous Dispersions in Presence of Water-Soluble Polymers, International Journal of Pharmaceutical Research, 2020, Vol. 12, Supplementary Issue 2, pp. 1821-1824.
17. O.A. Butusova. Stabilization of Carbon Microparticles by High-Molecular Surfactants, International Journal of Pharmaceutical Research, 2020, Vol. 12, Supplementary Issue 2, pp. 1147-1151.

18. Yu.V. Ioni. Synthesis of Metal Oxide Nanoparticles and Formation of Nanostructured Layers on Surfaces under Ultrasonic Vibrations, International Journal of Pharmaceutical Research, 2020, Vol. 12, Issue 4, pp. 3432-3435.
19. O.A. Butusova. Vinyl Ether Copolymers as Stabilizers of Carbon Black Suspensions, International Journal of Pharmaceutical Research, 2020, Vol. 12, Supplementary Issue 2, pp. 1152-1155.
20. B.A. Garibyan. Mechanical Properties of Electroconductive Ceramics, International Journal of Pharmaceutical Research, 2020, Vol. 12, Supplementary Issue 2, pp. 1825-1828.
21. B.A. Garibyan. Enhancement of Mechanical Properties of Inorganic Glass under Ultrasonic Treatment, International Journal of Pharmaceutical Research, 2020, Vol. 12, Supplementary Issue 2, pp. 1829-1832.
22. O.A. Butusova. Adsorption Behaviour of Ethylhydroxyethyl Cellulose on the Surface of Microparticles of Titanium and Ferrous Oxides, International Journal of Pharmaceutical Research, 2020, Vol. 12, Supplementary Issue 2, pp. 1156-1159.
23. A.N. Tarasova. Vibration-based Method for Mechanochemical Coating Metallic Surfaces, International Journal of Pharmaceutical Research, 2020, Vol. 12, Supplementary Issue 2, pp. 1160-1168.
24. N.A. Bulychev, A.V. Ivanov. Study of Nanostructure of Polymer Adsorption Layers on the Particles Surface of Titanium Dioxide, International Journal of Nanotechnology, 2019, Vol. 16, Nos. 6/7/8/9/10, pp. 356 – 365.
25. A.N. Tarasova. Effect of Reagent Concentrations on Equilibria in Water-Soluble Complexes, International Journal of Pharmaceutical Research, 2020, Vol. 12, Supplementary Issue 2, pp. 1169-1172.
26. Yu.V. Ioni. Effect of Ultrasonic Treatment on Properties of Aqueous Dispersions of Inorganic and Organic Particles in Presence of Water-Soluble Polymers, International Journal of Pharmaceutical Research, 2020, Vol. 12, Issue 4, pp. 3440-3442.
27. Bulychev, N.A., Rabinskiy, L.N. Ceramic nanostructures obtained by acoustoplasma technique//Nanoscience and Technology: An International Journal, 2019, 10 (3), p. 279–286.
28. Bulychev, N.A., Rabinskiy, L.N., Tushavina, O.V. Effect of intense mechanical vibration of ultrasonic frequency on thermal unstable low-temperature plasma// Nanoscience and Technology: An International Journal, 2020, 11 (1), p. 15–21.
29. Yu.V. Ioni, A. Ethiraj. New Tailor-Made Polymer Stabilizers for Aqueous Dispersions of Hydrophobic Carbon Nanoparticles, International Journal of Pharmaceutical Research, 2020, Vol. 12, Issue 4, pp. 3443-3446.
30. A.N. Tarasova. Effect of Vibration on Physical Properties of Polymeric Latexes, International Journal of Pharmaceutical Research, 2020, Vol. 12, Supplementary Issue 2, pp. 1173-1180.
31. B.A. Garibyan. Modelling of Technical Parameters of Discharge Reactor for Polymer Treatment, International Journal of Pharmaceutical Research, 2020, Vol. 12, Supplementary Issue 2, pp. 1833-1837.
32. Bulychev N. A., Kuznetsova E.L., Bodryshev V. V. Rabinskiy L.N. Nanotechnological aspects of temperature-dependent decomposition of polymer solutions, Nanoscience and Technology: An International Journal, 2018, Vol. 9 (2), p. 91-97.
33. Yu.V. Ioni, A. Ethiraj. Study of Microparticles Surface Modification by Electrokinetic Potential Measuring, International Journal of Pharmaceutical Research, 2020, Vol. 12, Issue 4, pp. 3436-3439.
34. N.A. Bulychev, M.A. Kazaryan. Optical Properties of Zinc Oxide Nanoparticles Synthesized in Plasma Discharge in Liquid under Ultrasonic Cavitation, Proceedings of SPIE, 2019, Vol. 11322, article number 1132219.
35. Yu.V. Ioni. Nanoparticles of noble metals on the surface of graphene flakes, Periodico Tche Quimica, 2020, Vol. 17, No. 36, pp. 1199-1211.
36. Formalev, V.F., Kartashov, É.M., Kolesnik, S.A. On the Dynamics of Motion and Reflection of Temperature Solitons in Wave Heat Transfer in Limited Regions // Journal of Engineering Physics and Thermophysics, 2020, 93(1), p. 10–15.
37. Formalev, V.F., Bulychev, N.A., Kuznetsova, E.L., Kolesnik, S.A. The Thermal State of a Packet of Cooled Microrocket Gas-Dynamic Lasers // Technical Physics Letters, 2020, 46(3), p. 245–248.
38. Astapov, A.N., Kuznetsova, E.L., Rabinskiy, L.N. Operating capacity of anti-oxidizing coating in hypersonic flows of air plasma // Surface Review and Letters, 2019, 26(2), 1850145 p.

39. Rabinskiy, L.N., Tushavina, O.V., Starovoitov, E.I. Study of thermal effects of electromagnetic radiation on the environment from space rocket activity // INCAS Bulletin, 2020, 12 (Special Issue), p. 141–148.
40. Babaytsev, A.V., Orekhov, A.A., Rabinskiy, L.N. Properties and microstructure of AlSi10Mg samples obtained by selective laser melting// Nanoscience and Technology: An International Journal, 2020, 11(3), p. 213–222.
41. Egorova, O.V., Kyaw, Y.K. Solution of inverse non-stationary boundary value problems of diffraction of plane pressure wave on convex surfaces based on analytical solution//Journal of Applied Engineering Science, 2020, 18(4), p. 676–680.